ELSEVIER

Contents lists available at ScienceDirect

Ultrasonics

journal homepage: www.elsevier.com/locate/ultras





Monitoring damage growth and topographical changes in plate structures using sideband peak count-index and topological acoustic sensing techniques

Guangdong Zhang a,b, Pierre A. Deymier a,c, Keith Runge a,c, Tribikram Kundu a,b,c,d,*

- ^a New Frontiers of Sound Science and Technology Center, University of Arizona, Tucson, AZ 85721, USA
- ^b Department of Civil and Architectural Engineering and Mechanics, University of Arizona, Tucson, AZ 85721, USA
- Department of Materials Science and Engineering, University of Arizona, Tucson, AZ 85721, USA
- ^d Department of Aerospace and Mechanical Engineering, University of Arizona, Tucson, AZ 85721, USA

ARTICLE INFO

Keywords: SPC-I technique Peri-ultrasound modeling Topological acoustic sensing Geometric phase change Structural health monitoring

ABSTRACT

Some topographies in plate structures can hide cracks and make it difficult to monitor damage growth. This is because topographical features convert homogeneous structures to heterogeneous one and complicate the wave propagation through such structures. At certain points destructive interference between incident, reflected and transmitted elastic waves can make those points insensitive to the damage growth when adopting acoustics based structural health monitoring (SHM) techniques. A newly developed nonlinear ultrasonic (NLU) technique called sideband peak count - index (or SPC-I) has shown its effectiveness and superiority compared to other techniques for nondestructive testing (NDT) and SHM applications and is adopted in this work for monitoring damage growth in plate structures with topographical features. The performance of SPC-I technique in heterogeneous specimens having different topographies is investigated using nonlocal peridynamics based peri-ultrasound modeling. Three types of topographies - "X" topography, "Y" topography and "XY" topography are investigated. It is observed that "X" and "XY" topographies can help to hide the crack growth, thus making cracks undetectable when the SPC-I based monitoring technique is adopted. In addition to the SPC-I technique, we also investigate the effectiveness of an emerging sensing technique based on topological acoustic sensing. This method monitors the changes in the geometric phase; a measure of the changes in the acoustic wave's spatial behavior. The computed results show that changes in the geometric phase can be exploited to monitor the damage growth in plate structures for all three topographies considered here. The significant changes in geometric phase can be related to the crack growth even when these cracks remain hidden for some topographies during the SPC-I based single point inspection. Sensitivities of both the SPC-I and the topological acoustic sensing techniques are also investigated for sensing the topographical changes in the plate structures.

1. Introduction

Nondestructive testing and evaluation (NDT&E) techniques using acoustic signals are widely used for structural health monitoring (SHM) to ensure the safety of structural components' operation [1,2]. Monitoring damages such as cracks in engineering structures is important and various well-established acoustic techniques can monitor damage growth in homogeneous structures. However, when damages or cracks appear in heterogeneous structures having various topographies the damage monitoring becomes much more challenging. For simplicity we will call such structures having various topographies as "topographical

structures". Topographical structures can be found in various engineering applications, such as in welded structures, or when thin-walled ductile metallic plate structures are bent, topographies of the welded and bent regions become different from the flat parts [3,4]. Topographies in structures can result in complex wave interactions arising from reflections and refractions causing negative wave interference when adopting acoustic wave-based monitoring techniques. When damage is generated in such topographical structures, the damage-induced information may remain hidden due to these negative or destructive interferences. Therefore, it would be of great interest to investigate the effect of topography on damage monitoring. Such investigation can

E-mail address: tkundu@arizona.edu (T. Kundu).

^{*} Corresponding author.

provide guidance for proposing optimal acoustics-based sensing techniques to detect and monitor damage growth in such engineering structures.

In recent years nonlinear ultrasonic (NLU) techniques have become more popular than conventional linear ultrasonic (LU) based techniques due to their high sensitivity in monitoring damages at their early stages [5]. A newly developed NLU technique called sideband peak count index (or SPC-I) has shown promising results for monitoring damages in different materials such as concrete [6-9], fiber reinforced polymer composites [10-12], metallic materials [5,13], fiber reinforced cement mortar [14,15] and additively manufactured metal parts [16,17]. In the SPC-I technique, sideband peaks are counted above a moving horizontal threshold line as this line moves between a preset lower limit and an upper limit in the spectral plot. The SPC-I values give the degree of nonlinearity associated for the inspected specimen – larger SPC-I values indicate higher nonlinearity. The SPC-I technique shows many advantages over other NLU techniques such as the two most popular and wellestablished techniques - higher harmonics generation (HHG) technique and nonlinear wave modulation spectroscopy (NWMS) method or frequency modulation (FM) method. For example, when adopting the HHG technique for guided waves propagating in plate structures, the guided wave mode selection criterion requires phase velocity and group velocity matching for the fundamental mode and the higher harmonic mode [18,19], and for many engineering materials with complex internal structures such as composites and concretes the higher order harmonic components do not appear thus making it difficult to apply this technique. The NWMS/FM technique can be applied regardless of the material geometry or the presence of reflecting boundaries and structural inhomogeneity. However, the two input wave frequencies for wave mixing need to be precisely controlled for optimal sideband generation, which means narrow band excitation is needed [20]. The SPC-I technique does not have such restrictions and hence is easier to implement, thus giving superiority of the SPC-I technique for damage monitoring.

In general, damage monitoring related problems are challenging due to their complexities and uncertainties. It is almost impossible to monitor damage growth accurately from the experimental data extracted from received ultrasonic signals at one receiver. For more complex topographical structures, it is very difficult to conduct parametric analysis experimentally. Hence, a good numerical modeling method which can simulate elastic waves propagating and interacting with damages producing linear and nonlinear response in complex structures such as topographical structures would be necessary. It can help us to understand the physical mechanism and provide useful guidance for practical experimental investigations [21]. Peri-ultrasound modeling which is based on nonlocal peridynamics theory [22,23] has shown advantages over other numerical modeling methods for modeling elastic wave propagation and its interaction with cracks, producing nonlinear response. Compared to finite element method (FEM) based modeling (spring model and activating/deactivating elements) [24,25] and finite difference-based method such as local interaction simulation approach or LISA [26,27], peri-ultrasound modeling can simulate nonlinear response from wave-crack interaction without changing cracks' surface properties artificially. It gives peri-ultrasound modeling advantages over other numerical methods. It should be noted that in finite element modeling when damage or crack sizes change, all meshes of elements and properties of cracked regions should be refreshed, element sizes become smaller, the number of elements increase rapidly, and it becomes challenging to artificially change the cracks' surface properties properly in these numerical methods. However, the mesh-free peri-ultrasound modeling does not have such restrictions since horizon size in peridynamics theory is directly related to the particle size, any change in the particle size changes the horizon size automatically.

Combining peri-ultrasound modeling and SPC-I technique the structural damages have been monitored successfully. The periultrasound modeling has been adopted for elastic wave propagating and interacting with cracks, thus producing nonlinear response in structures, and the SPC-I technique is then adopted as a nonlinear analysis tool to extract the nonlinear response from recorded periultrasound modeling signals. Hafezi and Kundu [28-30] initialed the peri-ultrasound modeling concept based on bond-based peridynamics for modeling elastic waves propagating and interacting with single crack in two-dimensional (2-D) plates, and nonlinear response was extracted with sideband peak count (SPC) technique – SPC plots for SPC-I analysis. It showed that thin cracks depict higher degree of nonlinearity than thick cracks and no cracks cases. Zhang et al [21,31] investigated nonlinear response for multiple cracks in three-dimensional (3-D) plate structures using ordinary state-based peri-ultrasound modeling. They showed the relations between crack size ("thin" and "thick" cracks) and the horizon size used in nonlocal peridynamics modeling. Similar nonlinear trends were observed for multiple cracks cases - the SPC-I values for thin cracks are larger than that for thick cracks and nocrack cases. Dynamic propagation process of cracks and its monitoring with SPC-I technique has been also investigated combining peridynamics and peri-ultrasound modeling. SPC-I shows an increasing trend at the initial stages of crack propagation (when only thin cracks are generated) and then SPC-I values start to decrease as the loading increases and thin cracks coalesce to form thick cracks [32]. These investigations provide evidence that on one hand peri-ultrasound modeling is a useful tool for modeling nonlinear interactions between elastic waves and cracks, and on the other hand, the SPC-I technique is a promising tool to extract crack-induced nonlinear response.

In this work the effect of increasing thickness of stationary cracks representing the damage growth in topographical plate structures is investigated. Three types of topography - "X" topography, "Y" topography and "XY" topography are considered in plate structures. Different topographical plate structures are formed by inserting thin strips of a second material in different directions. Letters "X", "Y" and "XY" indicate the distribution directions of these strips ("X" implies vertical strips are distributed along the horizontal direction or x-axis direction, similarly "Y" implies horizontal strips are distributed along the vertical direction or y-axis direction while "XY" implies vertical and horizontal strips are distributed in horizontal and vertical directions, respectively). The proposed peridynamics based peri-ultrasound modeling is adopted to simulate elastic waves propagating and interacting with cracks in these topographical plate structures. Nonlinear responses arising from wave-cracks interactions are captured and analyzed using the SPC-I technique to check the effect of different topographies on the crack detectability.

Recently some of us have introduced a method, topological acoustic sensing, which exploits changes in the geometric phase of acoustic waves to sense defects in some structure or environment. This method was originally developed to monitor, using seismic waves, changes in complex environments such as forests [33] or the state of permafrost in the arctic [34]. This method was extended to monitoring perturbations taking the form of (1) a mass defect located on an array of coupled acoustic waveguides [35], (2) mass defects in a nonlinear granular metamaterial [36] and, (3) a small subwavelength object on a flat surface submerged under water [37]. With this method, the state of the acoustic field in the unperturbed and perturbed cases are mapped as multidimensional vectors in an abstract complex space, a Hilbert space. The change in geometric phase due to perturbations is obtained by calculating the angle between those vectors. This angle represents a rotation of the state vector of the wave due to scattering by the perturbation. By exploiting sharp topological features spanned by the acoustic field multidimensional state vector, the geometric phase sensing modality can have higher sensitivity than magnitude-based sensing approaches. The effectiveness of the emerging topological acoustic sensing technique is also investigated for monitoring damage growth in topographical structures. Both SPC-I and topological acoustic sensing techniques are also used to monitor topographical changes in plate structures.

2. Theory and method

The nonlinear SPC-I analysis method and the topological acoustic sensing technique are briefly described here. The ordinary state-based (OSB) peri-ultrasound is adopted for modeling elastic waves propagating and interacting with cracks in topographical structures. The detailed theory and algorithm of OSB peri-ultrasound modeling can be found in the authors' previously published papers [21,31,32] and is omitted here. For the SPC-I analysis, only the important part is given here, many SPC-I related investigations both numerical and experimental can be found in the literature as mentioned in the introduction part so the readers can refer to them if interested. The emerging topological acoustic sensing technique for the topographical structure monitoring is also described in detail. Both SPC-I and geometric phase change-based sensing modality are adopted for monitoring damage growth in topographical plate structures.

2.1. Nonlinear SPC-I analysis method

Consider a spectral plot generated from a recorded signal as shown in the schematic diagram in Fig. 1a. The nonlinearities may be caused by damages or micro-cracks. Interactions between input elastic waves of different frequencies (major peaks in Fig. 1a) produce additional small peaks when propagating through nonlinear materials due to the frequency modulation effect as shown in the spectral plot. In the SPC-I analysis we are interested in counting the peaks generated by the modulation effect.

The SPC plot shown in Fig. 1b is generated by counting the peaks above a moving threshold line, shown by the horizontal continuous line in Fig. 1a. A threshold line (the horizontal continuous line) is moved vertically between two pre-set values which we call the lower threshold limit and upper threshold limit, shown by the dashed lines. When the moving threshold lime is varying vertically from the lower threshold limit to the upper threshold limit, all peaks shown by the circles that are above the moving threshold line are counted and plotted against the threshold value. The SPC plot (number of peaks as a function of the threshold value) gives a visual representation of the degree of material nonlinearity. A solid medium with high degree of nonlinearity should give higher SPC values compared to that for a linear elastic medium having a lower degree of nonlinearity.

The SPC-I is an index value which is the average of SPC values for all threshold positions. This index is a number that indicates the degree of material nonlinearity, higher the material nonlinearity, greater is this number. In this work, we adopt the SPC-I for investigating crack-induced nonlinear response in different types of topographical structures.

2.2. Topological acoustic sensing and geometric phase change

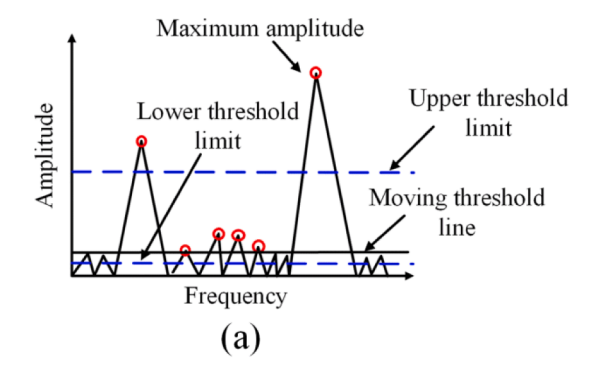
Topological acoustic sensing captures the change in the geometric phase of an acoustic field (linear and/or nonlinear) as its vectorial representation within a multidimensional Hilbert space rotated due to some perturbation. This phase is different from dynamic phase which is related to the phase accumulated by a wave as it travels at some speed along some path. The changes in vectorial representation of an acoustic field and its associated geometric phase relate to perturbation introduced in the reference system [38]. Previous studies adopted topological acoustic sensing [33–37] show that any simple change in the medium supporting an acoustic field may cause significant changes in geometric phase. When the topology of the manifold in the multidimensional space spanned by the vectorial representation of an acoustic fields exhibits sharp topological features such as twists, small changes in the medium supporting the acoustic field may lead to a sharp jump in geometric phase. Monitoring changes around such features leads to the high sensitivity of the geometric phase to small perturbations.

First, we consider the acoustic fields in the homogenous plates with and without damages to illustrate the process of topological acoustic sensing. Effectively, the vector representation of an acoustic field supported by a continuous plate lives in an infinite dimensional Hilbert space. To illustrate the method of topological acoustic sensing, we consider a much smaller discretized subspace to describe the acoustic field. This subspace is constituted of seven receiving points as shown in Fig. 2. It should be noted that at least two receiving points are needed to reflect the spatial characteristics of the acoustic field. More receiving points will improve the spatial resolution of the acoustic field and its geometry. Here, seven points are distributed symmetrically about the yaxis as shown in Fig. 2a (for the homogeneous plate without any cracks) and in Fig. 2b (for the homogeneous plate with two cracks). The geometric phase will change for the cracked plate compared to that with no crack case (reference state) because of the perturbations arising from these cracks. The thickness d of these two cracks takes values 0, 1, 2 and 4 mm for modeling damage growth in the plate. Plate having no crack is considered as the reference state or reference shape with respect to which the cracked cases are compared.

For the reference shape at each receiving location, we record the outof-plane velocity (in z direction) as a time series. Each of these seven time series are Fast Fourier transformed (FFT) to obtain complex amplitudes in the spectral domain. At a given frequency, these seven complex amplitudes can be represented as a normalized state vector in a seven dimensional complex Hilbert space. The 7 basis vectors of that subspace correspond to locations in the physical space. This normalized state vector can be written as [37],

$$C = \frac{1}{\sqrt{C_1^2 + C_2^2 + C_3^2 + ...C_7^2}} \begin{pmatrix} C_1 e^{i\phi_1} \\ C_2 e^{i\phi_2} \\ C_3 e^{i\phi_3} \\ ... \\ C_7 e^{i\phi_7} \end{pmatrix}$$
(1)

In equation (1), C_i and ϕ_i (i = 1, 2, 3...7) are magnitude and spatial phase at each receiving point. The components of this multidimensional state vector are the complex amplitudes of the field at every location in



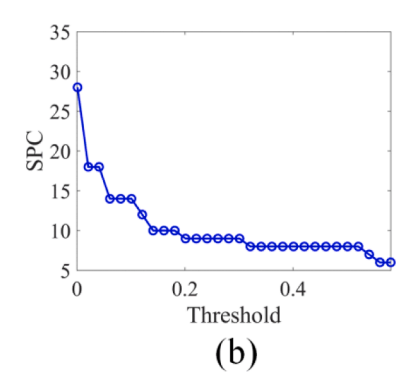
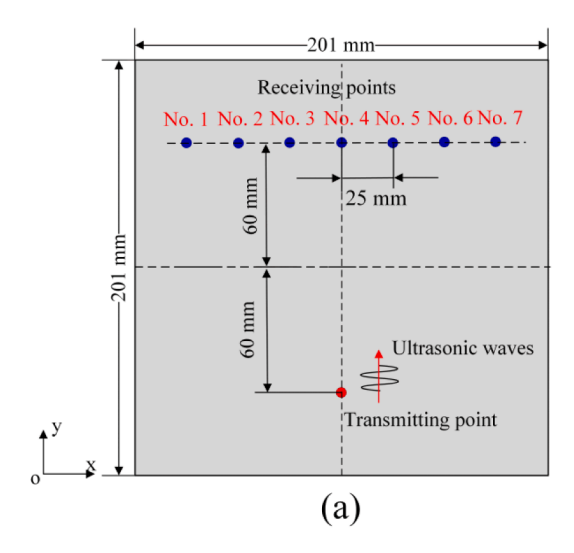


Fig. 1. Illustration of SPC. (a) Sideband peak counting and (b) example of SPC plot [21,31,32].



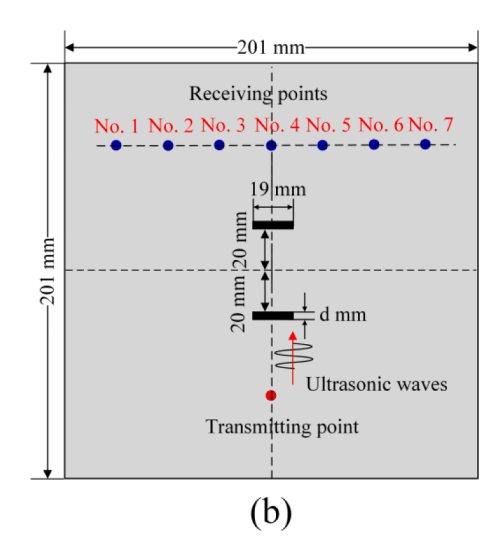


Fig. 2. 2-D view of the problem geometry for geometric phase sensing (a) crack-free reference state and (b) cracked plate - perturbed state.

the discretized space of the seven detectors. When cracks are introduced, the perturbation in the physical space scatters the acoustic waves and modifies the spatial distribution of the acoustic field. Perturbations such as cracks then change the normalized complex amplitude of the acoustic field to,

$$C' = \frac{1}{\sqrt{C_1'^2 + C_2'^2 + C_3'^2 + ...C_7'^2}} \begin{pmatrix} C_1'e^{i\phi_1'} \\ C_2'e^{i\phi_2'} \\ C_3'e^{i\phi_3'} \\ ... \\ C_7'e^{i\phi_7'} \end{pmatrix}$$
(2)

At a single given frequency f, the angle between the vector representation of the acoustic field along the 7 locations in the crack-free and cracked systems corresponds to a change in the geometric phase of the acoustic wave. This angle or single geometric phase change at the given frequency f can be obtained through the dot product of these two state vectors and can be expressed as,

$$\Delta \varphi = \arccos(\operatorname{Re}(C^* \bullet C')), \Delta \varphi \in [0, \pi]$$
(3)

where C^* denotes the complex conjugate of state vector C, and Re stands for the real part of a complex quantity.

Generally, the acoustic signals at each receiving point contain multiple frequencies, then a series of geometric phase changes can be plotted versus frequency. The spectral dependency of the geometric phase change $\Delta \varphi$ measures changes in the spatial characteristics of the acoustic field during wave propagation due to perturbations.

3. Model description

Plate structures containing two identical cracks with and without topographies are investigated and compared to examine the effect of topography on the detectability of cracks in plate structures using the SPC-I and topological acoustic sensing techniques. For the homogeneous plate or no-topography case, an isotropic aluminum plate is considered. Then topographical structures are formed by inserting thin strips of steel inserted in the aluminum plate, thus the topographical structure becomes heterogeneous. Three types of topographies – "X" topography, "Y" topography and "XY" topography are considered. "X" and "Y" topographies indicate that these strips are inserted and arranged along x-axis and y-axis directions, respectively. For the "XY" topography the strips are inserted in both x- and y-axes directions.

3.1. Homogeneous plate structure - Absence of any topography

In order to investigate the effect of topography on crack detection an aluminum plate structure containing cracks but without any topographical variation is first considered. The 2-D view (the xy plane) of the problem geometry of the aluminum plate structure with cracks but without topography is shown in Fig. 2b. The dimension of the plate structure is $201 \times 201 \times 3 \text{mm}^3$, and the aluminum material properties for numerical modeling are listed in Table 1 in section 3.2 along with the material properties of inserted steel strips. For wave propagation modeling, the vertical distances from the transmitting point and the receiving points to the x-axis are set at 60 mm, and seven receiving points are distributed symmetrically about the y-axis. In general, for most structural health monitoring applications generally one recorded signal by a strategically placed receiving sensor is analyzed by the SPC-I or some other analysis technique. However, for fair comparison with topological acoustic sensing technique, signal recorded at each receiving point is analyzed by the SPC-I technique in this investigation. Due to symmetries of these receiving points and wave propagation paths, only four propagation paths (path Nos. 1, 2, 3 and 4, or path Nos. 4, 5, 6 and 7) are analyzed by the SPC-I technique. Two identical cracks of length 19 mm and thickness d mm (d takes value 0, 1, 2 and 4 in this work) are considered for modeling damage growth. The two cracks are symmetrically placed about the x-axis and the closest vertical distances from the x-axis to the surface of the two cracks are 20 mm. The two cracks are also located symmetrically about the y-axis as shown in Fig. 2b.

In this work, in the peri-ultrasound modeling the entire plate structure is discretized into cubes with side length 1 mm, and cracks are formed by removing one or more layers of cubes from the plate structure. For example, each crack in Fig. 2b can be formed by removing d layers (where d takes values 0, 1, 2 and 4 to model cracks of different thicknesses) of cubes in the y direction and in each layer 19 cubes in the x direction, 3 layers in the z direction are removed to form throughthickness cracks. The horizon size is selected as $\delta = 3.015\Delta x$ following references [21,31,32] to ensure both computational efficiency and accuracy, where Δx is 1 mm which denotes the side length of a cube as mentioned above.

An Hanning window modulated excitation displacement field (see

Table 1
Material properties of aluminum and steel used in peri-ultrasound modeling.

Materials	Young's modulus (GPa)	Poisson's ratio	Density (kg/m³)
Aluminum	71.50	0.33	2700
Steel	220.00	0.30	7800

equation (4) is applied at the transmitting point to excite the structure in the negative z direction.

$$u(\mathbf{x},t) = u_0(\mathbf{x})\sin(2\pi f t)\sin^2\left(\pi \frac{t}{T}\right)$$
(4)

In equation (4), f is the central frequency of the ultrasonic wave which is 200 kHz, t is time and T is the total duration of the excitation which can control the number of cycles of the input excitation signal. x is a 3-D location vector that denotes the excitation point position at which the displacement field is applied (transmitting sensor position). u_0 is the applied or initial displacement amplitude that takes value 1×10^{-4} m in our peri-ultrasound modeling. The normalized time domain and frequency domain signals for the input or initial excitation are shown in Fig. 3.

At the receiving point, out-of-plane velocity fields (in the z direction) for each crack thickness are recorded at every calculation step to obtain the time history signal at each receiving point. Thus, seven signals are recorded at seven receiving points for crack thickness 0 mm (no crack), 1 mm, 2 mm and 4 mm. Then, SPC-I analysis and geometric phase change analysis are applied to these signals. The sampling frequency for recording the signals is 50 MSa/s (mega samples per second).

3.2. Heterogeneous plate structures

For the same plate structure dimensions shown in Fig. 2b, steel strips are inserted in aluminum matrix to form the heterogeneous topographical structure. Three types of topographies – "X" topography, "Y" topography and "XY" topography are considered as shown in Fig. 4.

The "X" topography shown in Fig. 4a consists of two pairs of steel strips (four strips) inserted and arranged in the x-axis direction in the aluminum plate. Both pairs of strips are symmetrically arranged about the y-axis. The "Y" topography shown in Fig. 4b includes three steel strips arranged in the y-axis direction and inserted in the aluminum plate, one of which is located at the center of the plate with its central line coinciding with the x-axis, and the other two are symmetrically distributed about the x-axis. The "XY" topography is simply the combinations of "X" topography and "Y" topography as shown in Fig. 4c. The width of the strips is 7 mm and length is 201 mm for all topographical plate structures. For wave propagation modeling, in these heterogeneous plates the transmitting and receiving point locations are taken the same as shown in Fig. 2. Seven receiving points are considered for both SPC-I and topological acoustic sensing analyses. The baselines for both SPC-I and geometric phase change sensing for these heterogeneous structures are the respective plates without any crack. Aluminum and steel properties for the peri-ultrasound modeling are shown in Table 1.

To have a better understanding of how elastic waves propagate in topographical structures, the phase velocity dispersion curves of 3 mm thick steel plate and aluminum plate are computed using the material properties given in Table 1. Fig. 5 shows these plots.

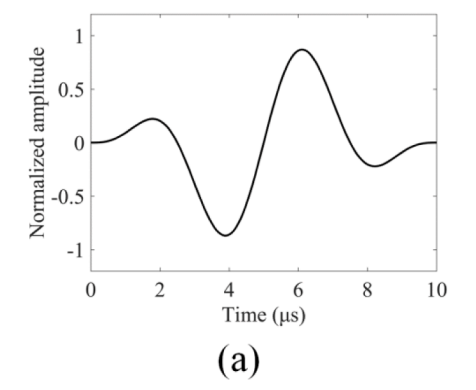


Fig. 5 shows that waves propagate a little faster in steel than in aluminum for both A_0 and S_0 guided wave modes at input central frequency of 200 kHz.

4. SPC-I sensing results for damage growth

4.1. Homogeneous aluminum plate structures

The peri-ultrasound modeling predicts wave motions over the entire 3-D problem geometry of the plate structure. Four cases with different crack thicknesses (0 mm, 1 mm, 2 mm and 4 mm) for the same crack length (19 mm) are numerically modeled. The snapshots of displacement magnitude fields at time steps 16 μs , 20 μs and 22 μs , for different crack thicknesses are shown in Fig. 6. These times are selected to show how elastic waves interact with these cracks as the wave fronts pass through the cracks.

It can be seen from Fig. 6 that peri-ultrasound modeling can successfully capture the wave propagation behaviors, and it also clearly shows the interactions between waves and cracks in the plate structures. At the seven receiving points, out-of-plane velocity fields for these four different crack thicknesses (0 mm, 1 mm, 2 mm and 4 mm) are recorded for further SPC-I analysis. We show four recorded signals at receiving point No. 4 (path No. 4) to illustrate how SPC-I works for damage monitoring. The time histories and corresponding spectral plots for the homogeneous aluminum plate are shown in Fig. 7.

Then we consider the spectral plots of Fig. 7b which are analyzed by the SPC-I technique. It has been reported in the authors' earlier publication [39] that not all peaks in spectral plots in Fig. 7b are affected by the nonlinear behavior of the material. The nonlinear response only affects the sideband peaks that are far away from the central excitation frequency while the main lobes around the central frequency capture the response due to the linear scattering. In general, sideband peak amplitudes are much lower than the main lobes (usually even much less than 10 % of the maximum amplitude) [21,28]. For high resolution sensing of the nonlinear response by the SPC-I technique, one should not set the upper limit of the moving threshold too high, especially for weak nonlinearity cases. For this reason, we took the threshold values varying from 0 to 12 % of the maximum peaks in each spectral plot in Fig. 7b for the SPC-I analysis. The SPC plots (the number of peaks above the threshold line as a function of the threshold value) for path No. 4 are shown in Fig. 8a. The SPC-I values are the average of SPC values for all threshold positions and are shown in Fig. 8b for the four paths. As mentioned before, the receiving points are distributed symmetrically about the y-axis so wave propagation paths are also symmetric. Therefore, for the SPC-I sensing four paths (either receivers No. 1, No. 2, No.3 and No. 4, or receivers No. 4, No. 5, No.6 and No. 7) are enough to show the effects of different levels of damage on the SPC-I variations along different paths. From the plotted SPC curves, the SPC-I values for threshold varying from 0 to any upper limit (which is less than or equal

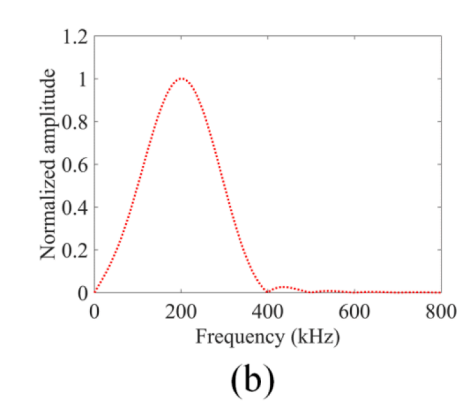


Fig. 3. Normalized initial or input excitation. (a) Time domain signal and (b) frequency domain signal.

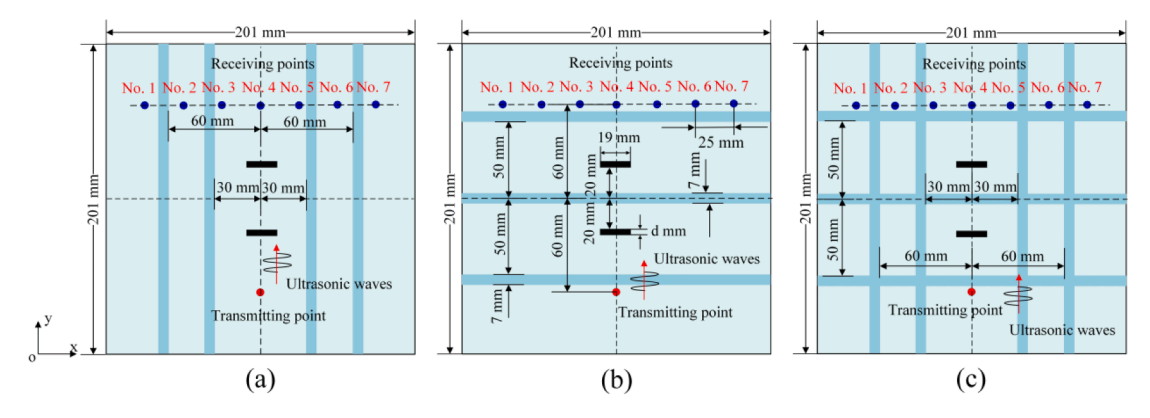


Fig. 4. 2-D views of aluminum plates containing steel strips and two cracks - (a) "X" topography, (b) "Y" topography and (c) "XY" topography.

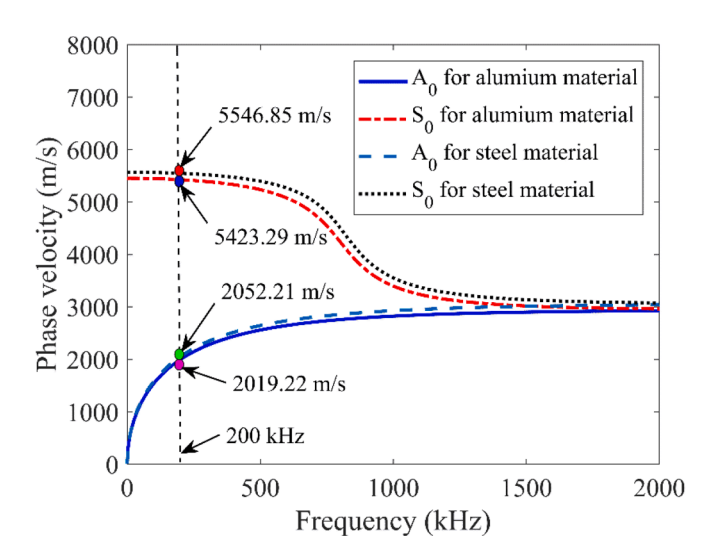


Fig. 5. Phase velocity dispersion curves for $3\ \mathrm{mm}$ thick aluminum and steel plates.

to 12 %) for all four paths can be generated. The damage growth information can be visualized graphically in SPC plots and here we show an example of SPC-I values with threshold varying from 0 to 12 % in Fig. 8b and from 0 to 8 % in Fig. 8c for comparison. It can be seen that similar trends are observed for crack induced nonlinearity for path number 4 that is affected most by the cracks which are located on this path. In the rest of the paper, the upper limits of thresholds are set at 12 % of the peak value for the SPC-I analysis.

First, it can be seen that the SPC-I parameters are path-dependent – different propagation paths produce different SPC-I values and trends. For paths No. 1 and No. 2, SPC-I values do not vary much when the crack thickness increases. This is because these two paths are far away from the cracks shown in Fig. 2b and hence are not significantly affected by the cracks. Similar phenomena have been reported in the literature [40] when adopting relative acoustic nonlinearity parameter (RANP) for characterizing fatigue cracks using active sensor networks with Lamb waves. It was found that when sensing paths are away from cracks, the RANP decreases and then remains constant (thus, no nonlinearity is detected). For paths No. 3 and No. 4 the trends are different, SPC-I first shows an increasing trend up to 2 mm thick crack, and then starts to decrease for both paths. The SPC-I variation is stronger for path No. 4 than path No. 3. This is because along path No. 4 the highest degree of damage-induced nonlinearity is sensed since this path goes through the crack. In several experimental and theoretical investigations this trend of SPC-I variation – first increasing and then decreasing, thus forming a hump has been reported [8-10,12,21]. Such hump in the SPC-I plot indicates the nonlinearity reaching the maximum value because of the

highest density of micro-crack accumulation and then the SPC-I value starts to decrease as the micro-cracks coalesce to form macro-cracks. Thus, such hump in the SPC-I plot can serve as a warning sign for macro-crack formation as well as damage detection. In our modeling thicker cracks represent macro-cracks while thinner cracks are representative of micro-cracks since the acoustic energy can pass through the thinner cracks but not thicker cracks.

4.2. Heterogeneous aluminum plate structures

When steel strips are inserted in aluminum matrix, the plate becomes heterogeneous. SPC-I sensing results from different sensing paths for different topographies – "X" topography, "Y" topography and "XY" topography are shown in this section.

4.2.1. "X" topography

Wave propagation snapshots for "X" topography in aluminum matrix plate structures at times $16~\mu s$, $20~\mu s$ and $22~\mu s$ are shown in Fig. 9.

Following the same SPC-I analysis steps discussed in section 4.1, the SPC plots from the recorded signals of path No. 4 are generated and shown in Fig. 10a and SPC-I variations for four paths are shown in Fig. 10b.

It can be seen that when "X" topography is considered, for all four paths no expected trend (humps) for SPC-I variations is observed which can indicate that damage growth cannot be detected in this case. Thus "X" topography can hide damages in plate structures.

4.2.2. "Y" topography

For plates having "Y" topography, wave propagation snapshots at times $16 \mu s$, $20 \mu s$ and $22 \mu s$ are shown in Fig. 11.

The SPC plots generated from the recorded signals for path No. 4 are shown in Fig. 12a and SPC-I variations for four paths are shown in Fig. 12b.

The expected SPC-I trend – its value increasing up to 2 mm thick crack and then decreasing, thus forming a hump, is observed for wave propagation path No. 4. This observation is consistent with homogeneous aluminum plate case given in Fig. 8b. Therefore, it indicates that "Y" topography in plate structures does not affect the damage growth monitoring capability of the SPC-I technique.

4.2.3. "XY" topography

Similarly, snapshots at times 16 $\mu s, 20~\mu s$ and 22 μs for the plate structure with "XY" topography are shown in Fig. 13, and the SPC plots from the recorded signals of path No. 4 are shown in Fig. 14a and the SPC-I variations for four paths are shown in Fig. 14b.

From Fig. 14b, it can be again seen that damage growth cannot be detected very clearly using the SPC-I sensing technique for the plate with "XY" topography. Therefore, "XY" topography can also hide damages in plate structures.

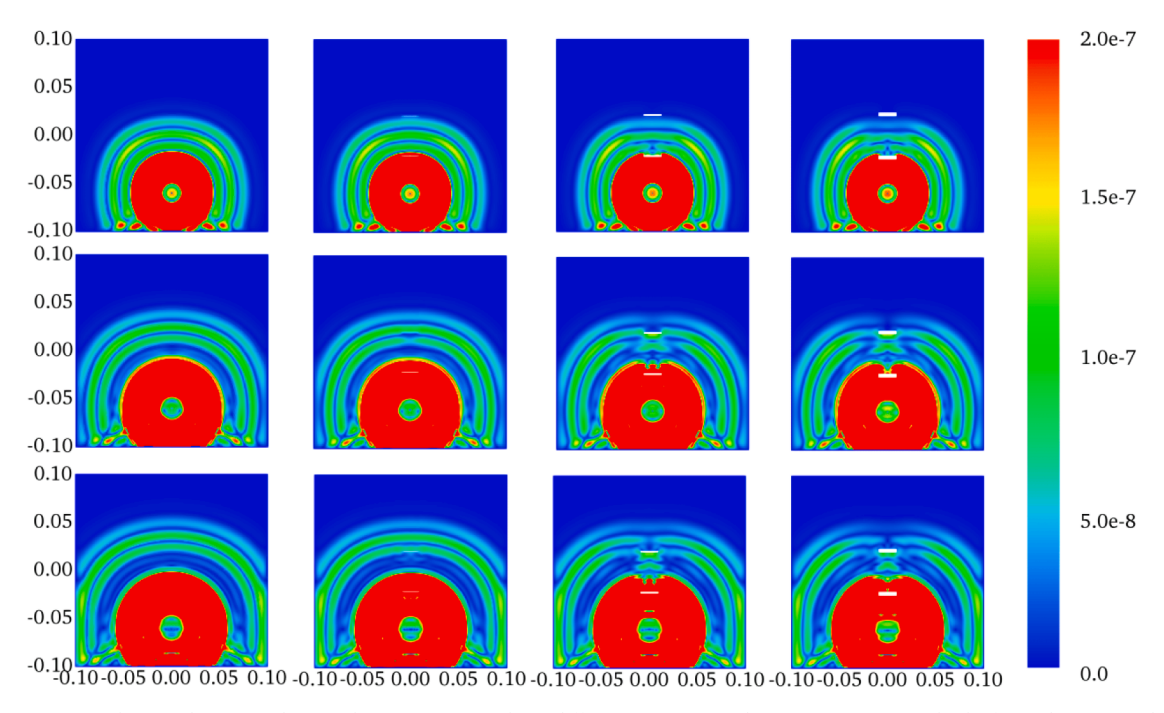


Fig. 6. Wave motion snapshots in aluminum plates without any topography at different times in (1) plate containing no crack (the first column), (2) plate containing two 1 mm thick cracks (the second column), (3) plate containing two 2 mm thick cracks (the third column) and (4) plate containing two 4 mm thick cracks (the right column). Plots from top to bottom rows show wave fronts at times 16 μs, 20 μs and 22 μs.

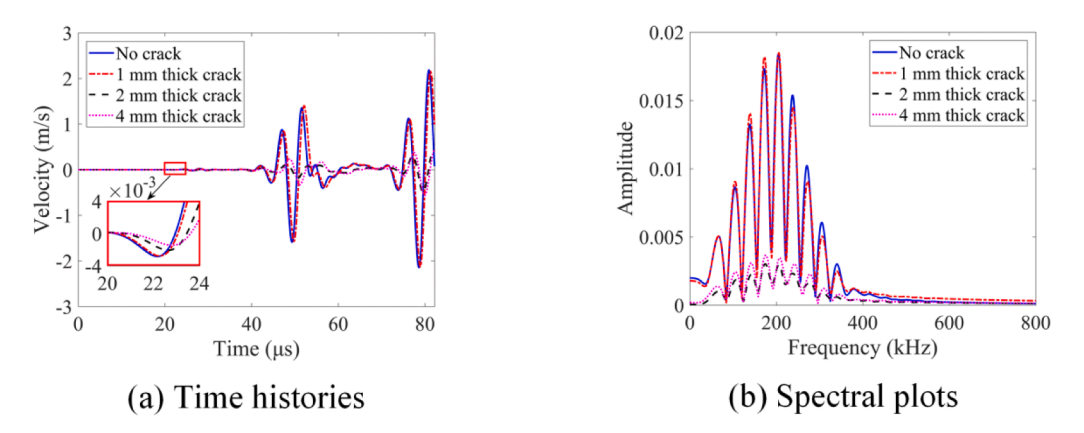


Fig. 7. Time histories and spectral plots for out-of-plane velocity fields in z direction at receiving point No. 4 in the homogeneous aluminum plate.

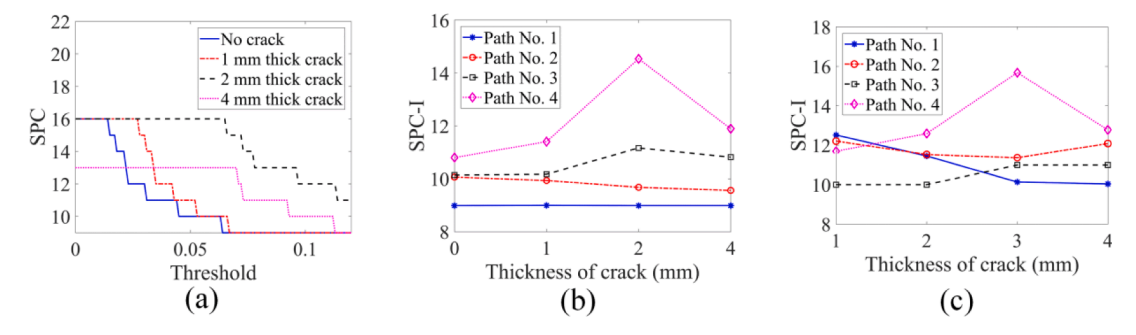


Fig. 8. For the homogeneous aluminum plate, shown in Fig. 2b, containing two cracks of different thicknesses -0 mm (no crack), 1 mm, 2 mm and 4 mm, the SPC plots with threshold varying from 0 to 12 % of the maximum amplitudes of each spectral plot obtained from path No. 4 are shown in Fig. 8(a), the SPC-I variations for four paths (No. 1, No. 2, No. 3 and No. 4) with threshold varying from 0 to 12 % are shown in Fig. 8(b) and the SPC-I variations for four paths (No. 1, No. 2, No. 3 and No. 4) with threshold varying from 0 to 8 % are shown in Fig. 8(c).

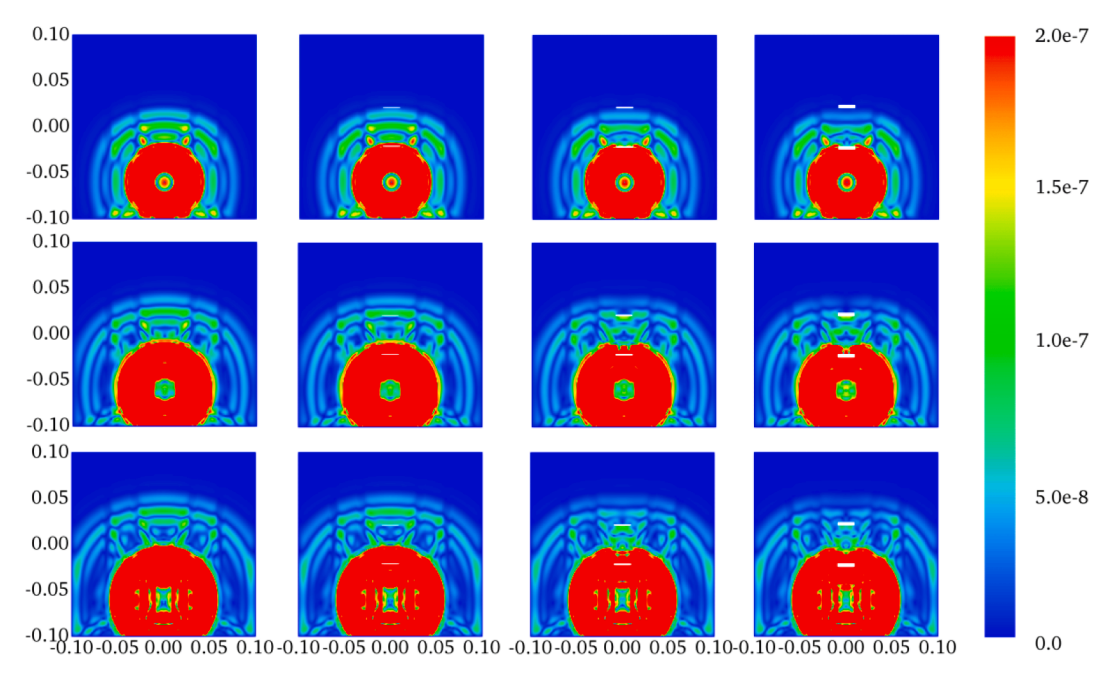


Fig. 9. Wave motion snapshots in aluminum matrix plate structures with "X" topography at different times, (1) structure containing no crack (the first column), (2) structure containing two 1 mm thick cracks (the second column), (3) structure containing two 2 mm thick cracks (the third column) and (4) structure containing two 4 mm thick cracks (the right column). Plots from top to bottom rows show wave fronts at times $16 \mu s$, $20 \mu s$ and $22 \mu s$.

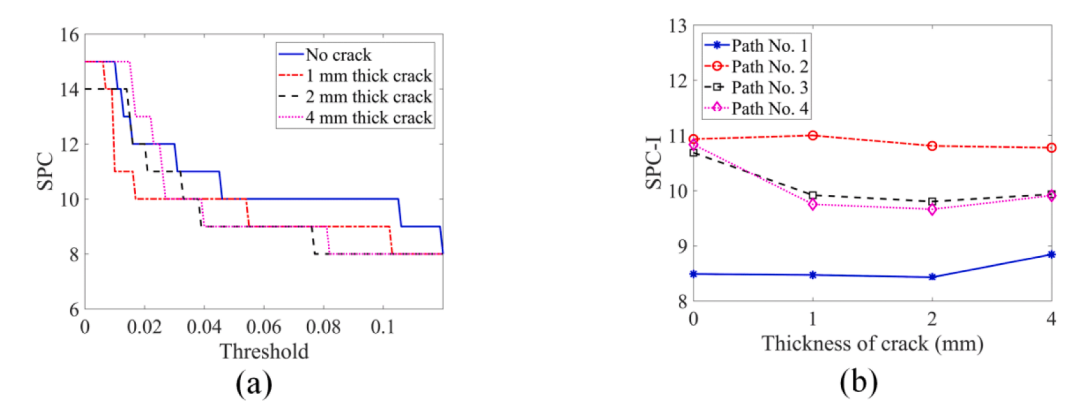


Fig. 10. For the plate containing two cracks of different thicknesses and having "X" topography (vertical steel strips in an aluminum plate as shown in Fig. 4a) the SPC plots generated from path No. 4 are shown in Fig. 10(a) and the SPC-I variations for the four paths are shown in Fig. 10(b).

From the SPC-I sensing results for damage growth in both homogeneous and heterogeneous structures, it can be concluded that "X" and "XY" topographies can hide cracks or make them undetectable while "Y" topography does not affect the damage monitoring capability when SPC-I technique is used. Crack hiding phenomenon for "X" and "XY" topographies can be explained from the wave propagation plots presented above that show how wave energy interacts with cracks (see Figs. 6, 9, 11 and 13) as the wave passes through cracks. The existence of "X" topography and "XY" topography in plate structures results in destructive interference between reflected waves from steel strips' boundary and the propagating wave from the source. After these mixed waves pass through cracks wave fronts cannot keep their perfect shapes and are made up of several scattered clusters as shown in Figs. 9 and 13, and such scattered wave energy can cause nonlinear information lost at the receiving points making it difficult to monitor the damage growth. For homogeneous plate and the plate with "Y" topography, the wave front shape is disturbed less by such scattered energy after passing through cracks as shown in Figs. 6 and 11. Hence, for these two cases, the nonlinear information generated by the cracks is preserved in the propagating wave front and is recorded by the receivers making the damage growth detectable. Appendix A gives the SPC-I sensing results for damage growth in steel plates with aluminum strips. In this case, the material properties of matrix and strips are simply interchanged. Similar phenomenon is observed – "X" and "XY" topographies make cracks undetectable by the SPC-I technique while the cracks are detectable in homogeneous and heterogeneous plates having "Y" topography, as expected.

5. Topological acoustic sensing results for damage growth

The damage growth monitoring results with topological acoustic sensing are presented in this section for both homogeneous and heterogeneous aluminum plates. Geometric phase changes are obtained from reference state vectors (crack-free plates) and perturbed state vectors from cracked plates for both homogeneous and heterogeneous aluminum plates. The effect of the crack growth in a homogeneous aluminum plate on the geometric phase change variation is shown in Fig. 15.

The crack growth effects on the geometric phase change for plates having different topographies (X, Y and XY) are shown in Fig. 16.

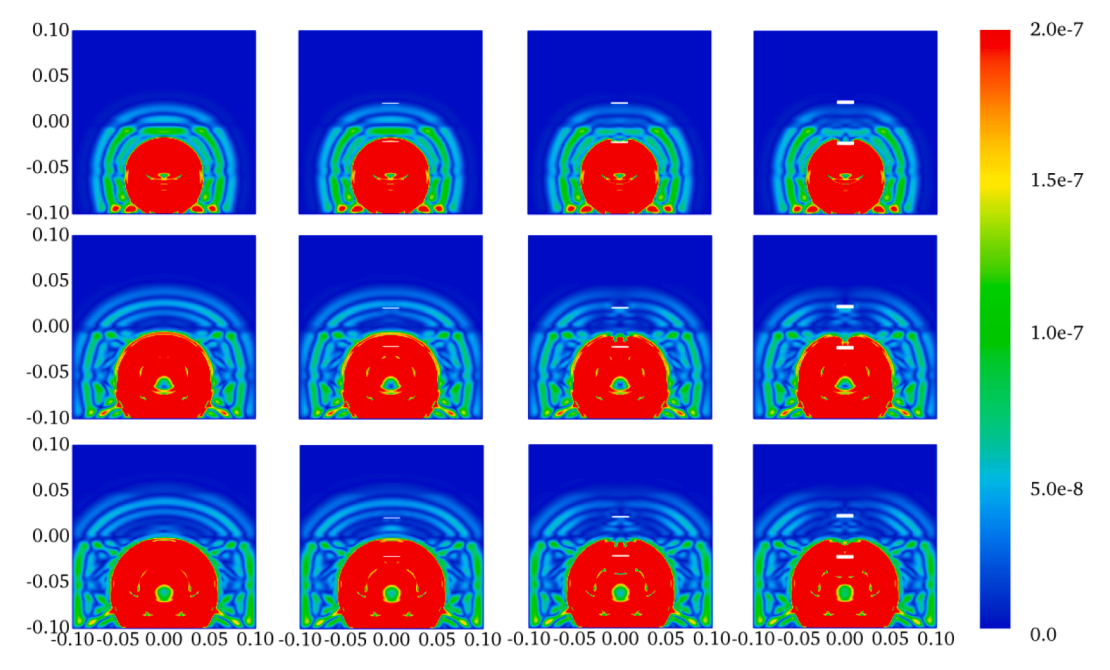


Fig. 11. Wave motion snapshots in plate structures with "Y" topography at different times (1) structure containing no crack (the first column), (2) structure containing two 1 mm thick cracks (the second column), (3) structure containing two 2 mm thick cracks (the third column) and (4) structure containing two 4 mm thick cracks (the right column). Plots in top to bottom rows show wave fronts at times $16 \mu s$, $20 \mu s$ and $22 \mu s$.

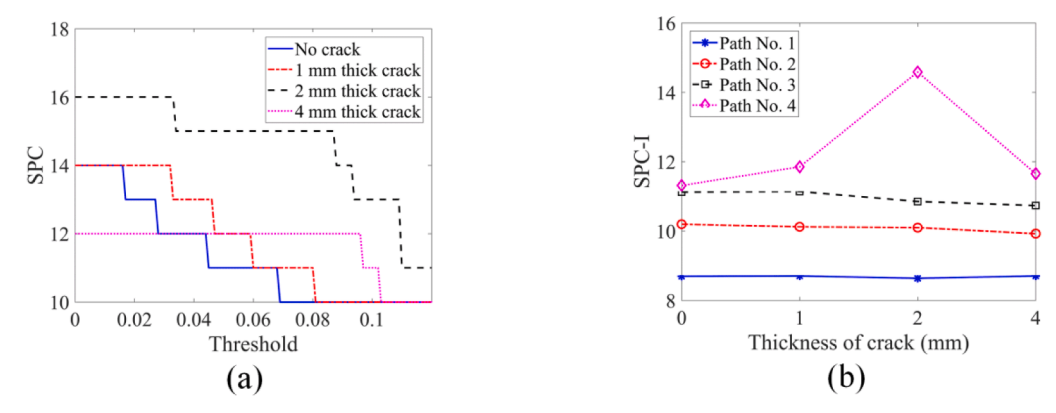


Fig. 12. For the plate containing two cracks of different thicknesses and having "Y" topography (horizontal steel strips in an aluminum plate as shown in Fig. 4b) the SPC plots from path No. 4 are shown in Fig. 12(a) and the SPC-I variations for four paths are shown in Fig. 12(b).

In all plots shown in Figs. 15 and 16 one can see that the introduction of cracks and crack thickness variations have a strong effect on $\Delta \phi$ (the geometric phase change) for both homogeneous and heterogeneous plates. At certain frequencies the $\Delta \varphi$ change is much stronger and show sharp peaks and dips compared to other frequencies. At higher frequencies (above 400 kHz) the oscillations die down. However, $\Delta \phi$ can still distinguish between no crack, 1 mm thick crack and 2 mm thick crack cases. However, no significant difference between 2 mm and 4 mm thick cracks is noticed. It has been also shown here (see Fig. 8b) and in previous investigations [7,10,31] that SPC-I technique is more effective in sensing the initial stages of damage growth (micro-damages). At higher frequencies (for example beyond 350 kHz in Fig. 15), $\Delta \varphi$ is showing similar trends – first increasing for up to 2 mm crack thickness and then decreasing. This is because at higher frequencies the wavelength is smaller. When the thickness of a crack increases from 2 mm to 4 mm, the nonlinear response decreases for smaller wavelengths. This is because for propagating waves having smaller wavelengths the two surfaces of a thick crack remain well-separated and do not interact to generate the nonlinear effect. However, for lower frequency waves having larger wavelengths the two surfaces of even a thick crack interact

producing nonlinear response.

Comparison of Figs. 15 and 16 also show that "Y" topography in aluminum plate structures does not significantly affect the damage detection sensitivity since the "Y" topography results (Fig. 16b) are like the no topography case (Fig. 15). One can notice that for "X" topography and "XY" topography (Fig. 16a and 16c) the $\Delta\phi$ curves are closer while for the homogeneous plate (Fig. 15) and for "Y" topography (Fig. 16b) cases the curves are closer and quite different from the other two topographies. We have seen earlier in sections 4.2.1 and 4.2.3 that SPC-I does not sense the nonlinear response due to the crack growth for "X" and "XY" topographies and hence these cracks can remain hidden for these two topographies if the SPC-I technique is adopted for their detection.

In Appendix A the topological acoustic sensing results for damage growth in steel plates with aluminum strips are shown. It can be seen from topological acoustic sensing results that for both homogeneous and heterogeneous steel plates at several frequencies there are sharp jumps forming multiple peaks and dips in geometric phase change plots. Such sharp oscillations are also observed in spectral plot of the received signal (see Fig. 7b). These oscillations are caused by constructive and

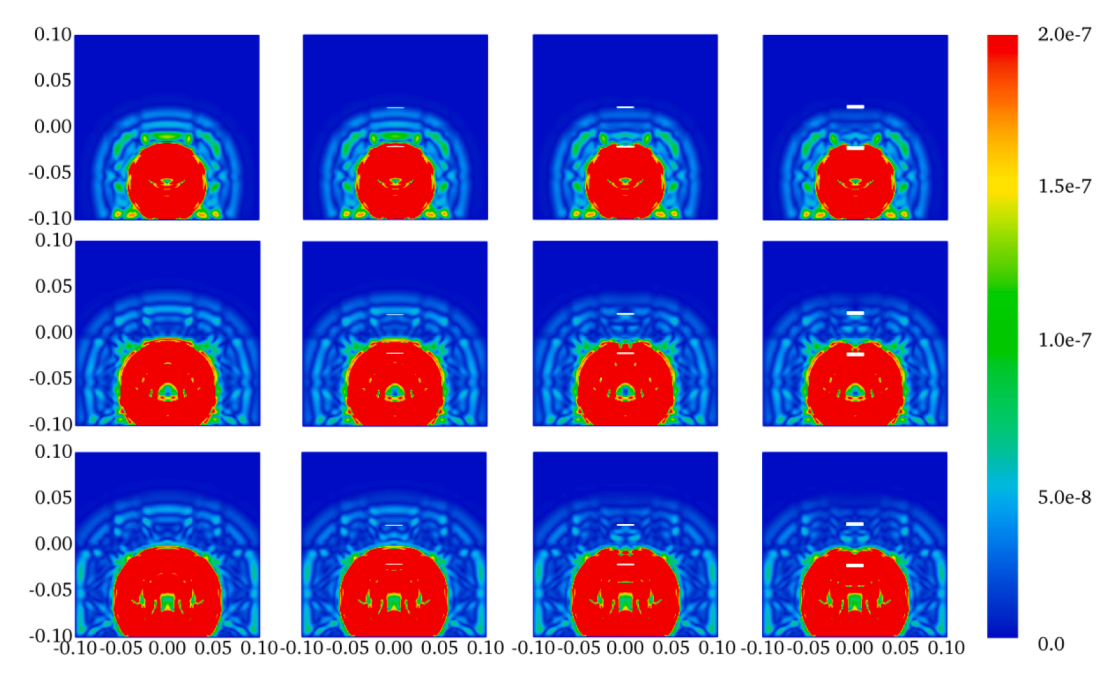


Fig. 13. Wave motion snapshots in plate structures with "XY" topography at different times (1) structure containing no crack (the first column), (2) structure containing two 1 mm thick cracks (the second column), (3) structure containing two 2 mm thick cracks (the third column) and (4) structure containing two 4 mm thick cracks (the right column). Plots in top to bottom rows show wave fronts at times $16 \mu s$, $20 \mu s$ and $22 \mu s$.

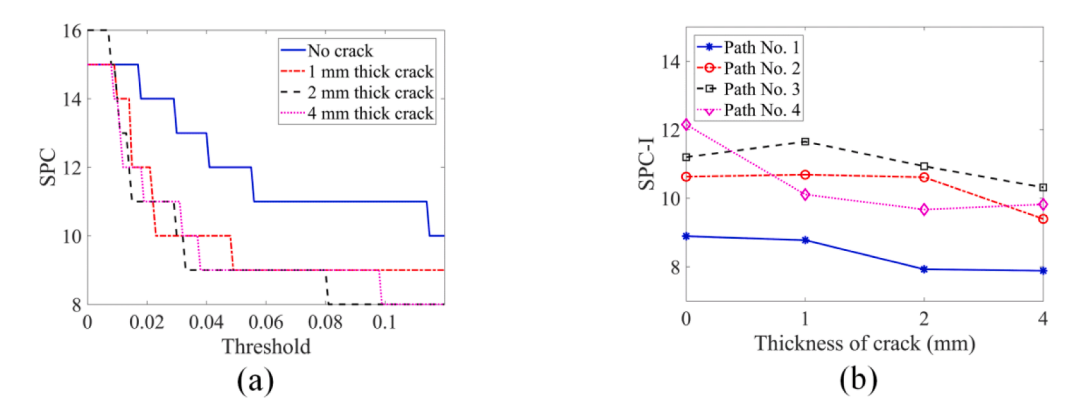


Fig. 14. For the plate containing two cracks of different thicknesses and having "XY" topography (both horizontal and vertical steel strips in an aluminum plate as shown in Fig. 4c) – the SPC plots for path No. 4 are shown in Fig. 14(a) and the SPC-I variations for four paths are shown in Fig. 14(b).

destructive interferences between the incident wave and the reflected waves from the plate boundary. For "X" topography and "XY" topography some reflected waves are also generated by the vertical strips in addition to the reflections from the plate boundary and hence the spectral patterns significantly change for these two topographies. The magnitudes of jumps vary as the crack thickness increases which can be used as a good parameter for monitoring the damage evolution.

6. Sensing topographical change of plates

So far, monitoring damage growth in homogeneous and heterogeneous plate structures (either aluminum or steel plates) using SPC-I technique and topological acoustic sensing technique has been investigated. In this section, it is investigated if the topographical change applied to a homogeneous plate can be detected by the SPC-I and geometric phase change techniques.

We first investigate the SPC-I variations for different topographies (no topography or homogeneous plate, "X" topography, "Y" topography and "XY" topography) in an aluminum plate containing no cracks. For topological acoustic sensing, the theory and methodology are the same

as illustrated in section 2.2. The reference state here is the homogeneous aluminum plate as shown in Fig. 17a, and the perturbed systems are heterogeneous aluminum plates as shown in Fig. 17b ("X" topography is shown as an example).

The sensing results with SPC-I and geometric phase change for different topographies in aluminum plates are shown in Fig. 18. The SPC-I variations are calculated from recorded signals along path No. 4 for homogeneous and heterogeneous plates.

It can be seen from Fig. 18a that the SPC-I values do not show much change between homogeneous and heterogeneous aluminum plates. This is because SPC-I mostly measures nonlinear response, and the change in topographies does not introduce any nonlinearity in the plate response. Small changes that are observed are mainly due to the changes in linear scattered fields which comes from the constructive and destructive interferences in the recorded signals, and the SPC-I technique captures this change in the linear scattered field. However, for geometric phase change results shown in Fig. 18b there are clear distinctions among different topographies. The levels of offset from reference horizontal solid line at the frequency range 0 to 500 kHz shown in the figure indicate the effect of various topographies. There are also

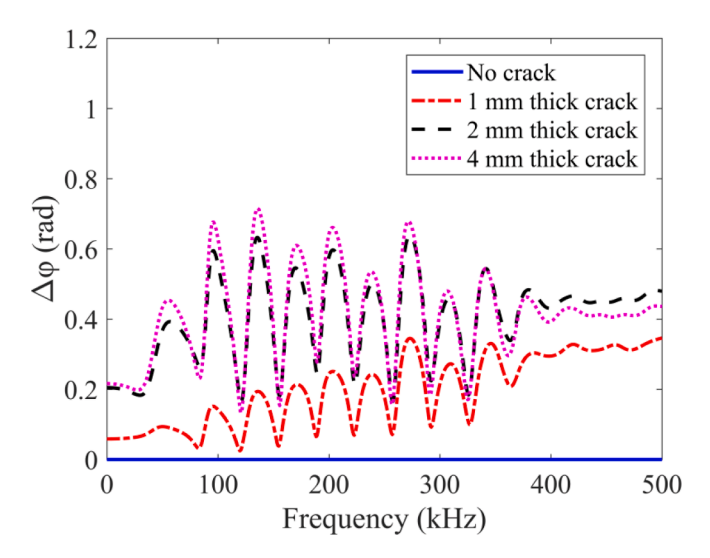


Fig. 15. Geometric phase change as a function of frequency as the crack thickness increases in the homogeneous aluminum plate.

sharp jumps at several frequencies, especially for "X" and "XY" topographies, indicating which frequencies are most sensitive for detecting these topographical changes. Appendix B gives the results for topographical changes when the material properties of matrix and strips are interchanged. Once again, there is not much differences in the SPC-I values for these topographies as can be seen in Appendix B, Much

stronger changes, especially for "X" and "XY" topographies are observed in geometric phase changes results shown in Appendix B.

7. Discussions and conclusions

In this work, monitoring damage growth in complex topographical plate structures is investigated using both SPC-I and topological acoustic sensing techniques. Three types of topographies – "X" topography, "Y" topography and "XY" topography are considered to convert a homogenous plate to a heterogeneous plate. Peridynamics based peri-ultrasound modeling is adopted for modeling elastic waves propagating and interacting with different thicknesses of cracks (modeling damage growth) in these topographical structures with and without cracks. For a single transmitter-detector pair aligned across the crack, the SPC-I sensing technique, finds that "Y" topography does not significantly affect the damage detection sensitivity while for "X" and "XY" topographies the SPC-I does not show expected variation for crack growth detection and the cracks can remain hidden. The SPC-I technique does not detect the three topographies for the intact plate. Geometric phase changes, however, can be used for monitoring those hidden cracks in topographical structures. For all three topographical structures the magnitudes of jumps in $\Delta \phi$ increase with crack thicknesses for all three topographies - "X", "Y" and "XY" at several frequencies. The relative changes of these jumps are big enough to distinguish these cracks and thus making these cracks detectable and their growths monitorable. The topological acoustic sensing technique can overcome the difficulties associated with the crack monitoring in heterogeneous structures with "X" and "XY" topographies. This is because it analyzes signals recorded

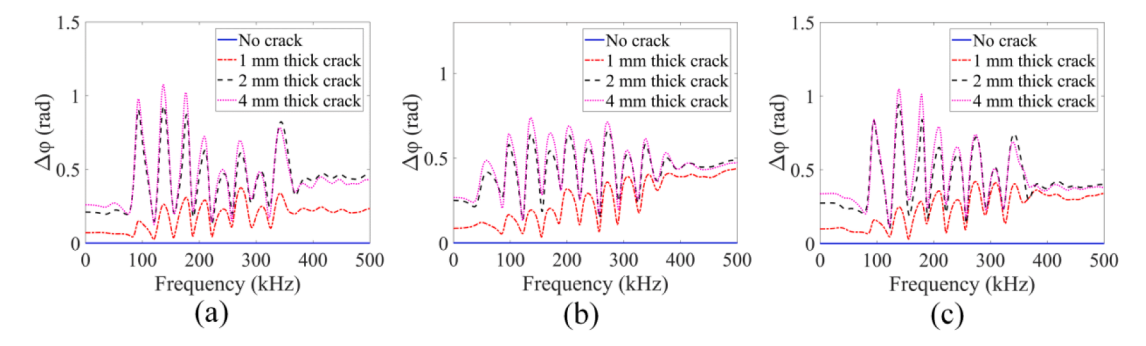


Fig. 16. Geometric phase changes as a function of frequency as the crack thickness increases in plates having (a) "X" topography, (b) "Y" topography and (c) "XY" topography.

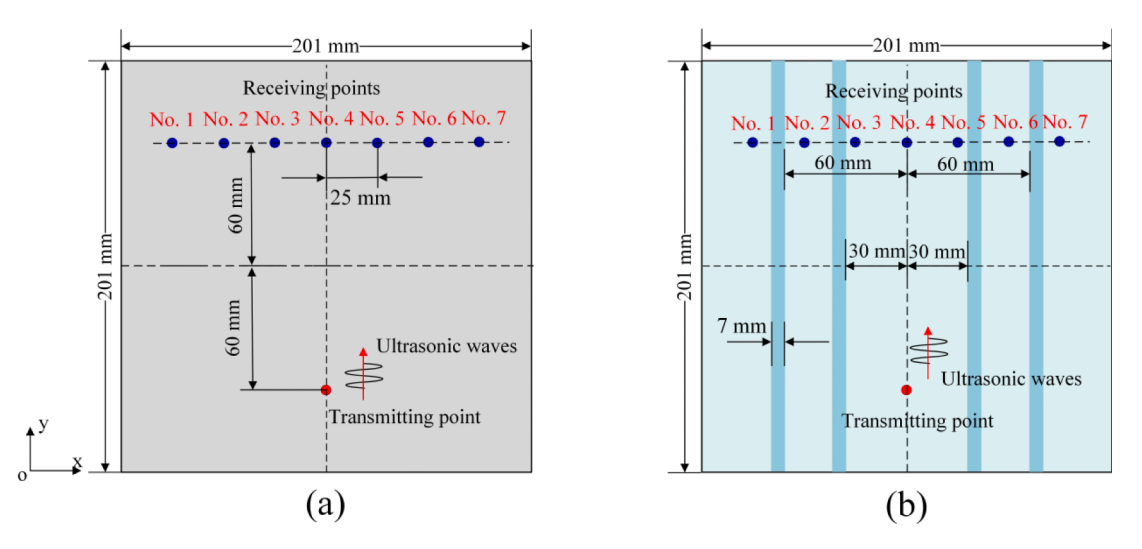
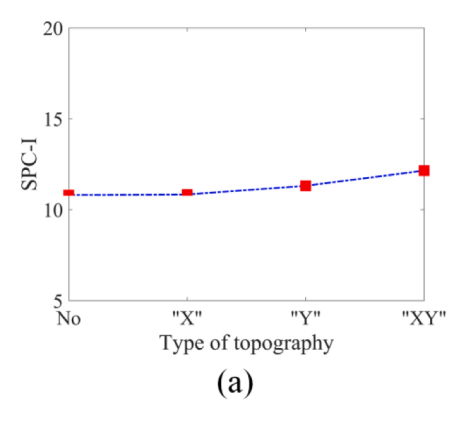


Fig. 17. 2-D view of geometries for acoustic sensing of topographical change (a) reference geometric shape and (b) perturbations to reference geometric shape due to "X" topography.



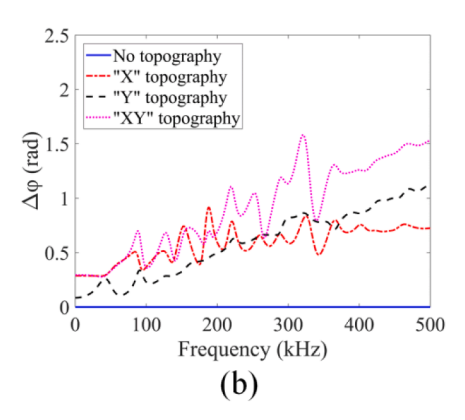


Fig. 18. Sensing results for different topographies in aluminum plates (a) SPC-I variations and (b) geometric phase changes.

by many sensors over a wide frequency range while the SPC-I technique only analyzes signals recorded at one receiver. Another reason for the success of the topological acoustic sensing technique is that it analyzes the changes of geometric phase in a multidimensional Hilbert space while the SPC-I technique mostly investigates the nonlinear response from the spectral plots. Thus in topological acoustic sensing we compare the geometric phase change in higher dimensional Hilbert space calculated from multiple sensing data instead of monitoring a parameter in time or frequency domain plots at a single sensing station.

The observations of cracks are hidden in "X" and "XY" types of topographies can be explained from the perspective of wave energy-crack interaction shown in the snapshots of the displacement fields at different times. Homogeneous plates and "Y" topography do not destroy wave front shapes at receiving points. However, for "X" topography and "XY" topography the destructive interference between the scattered (reflected and refracted fields) and the incident field make wave front shape severely distorted thus causing the loss of nonlinear information carried by the propagating waves at the receiving points. Thus cracks can remain undetectable in the SPC-I sensing technique. Results of geometric phase change also show that the "Y" topography results are similar to the no-topography case (homogeneous plate). However, for "X" topography and "XY" topography the $\Delta \phi$ variation patterns change from the homogeneous plate and "Y" topography cases. It can also help explain why "Y" topography in plate structures does not significantly affect the damage detection sensitivity for the SPC-I technique.

Both the SPC-I and the topological acoustic sensing techniques are also adopted for investigating their sensitivity to different topographical changes. It is found that SPC-I does not show strong variations for these topographical changes since SPC-I mainly measures nonlinear response in structures, and the introduction of topographical change does not introduce any nonlinearity in the structural response. For different topographies in plate structures, geometric phase changes show obvious distinctions since this parameter captures any linear or nonlinear spatial behavior change in the wave propagation field, and any perturbation in the spatial behavior can cause changes in geometric phase with high sensitivity at certain frequencies.

This work is useful for monitoring the damage growth in complex topographical structures. For some topographies the damage growth can remain hidden to the SPC-I technique with single transmitter–receiver

pair. However, geometric phase change obtained from multiple receivers can detect those cracks and monitor their growth with high sensitivity. The peri-ultrasound modeling results combining geometric phase change and SPC-I techniques can provide a strong crack detection tool and new insights in experimental investigation for structural health monitoring of topographical structures. Future work will investigate the sensitivity of the topological acoustic sensing approach to the number of detection sites and their location with respect to topographical features and/or defects.

CRediT authorship contribution statement

Guangdong Zhang: Writing – original draft, Visualization, Validation, Software, Resources, Methodology, Investigation, Formal analysis, Data curation. Pierre A. Deymier: Writing – review & editing, Methodology, Funding acquisition, Conceptualization. Keith Runge: Validation, Supervision, Resources. Tribikram Kundu: Writing – review & editing, Validation, Project administration, Methodology, Funding acquisition, Conceptualization.

Declaration of competing interest

The authors declare that they have no known competing financial interests or personal relationships that could have appeared to influence the work reported in this paper.

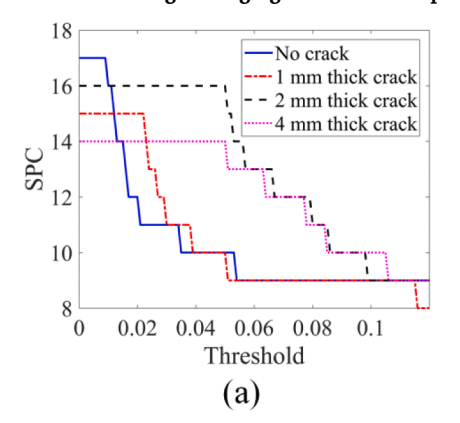
Data availability

Data used in the article is available upon reasonable request.

Acknowledgements

This work is partially supported by the National Science Foundation sponsored "New Frontiers of Sound Science and Technology Center" at the University of Arizona (Grant No. 2242925). Some financial support provided by the Central South University (CSU) in China towards the first author's stay at the University of Arizona is also gratefully acknowledged.

Appendix A. Results of sensing damage growth in steel plates with aluminum strips



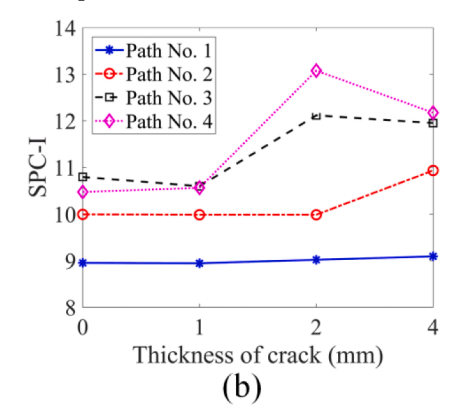
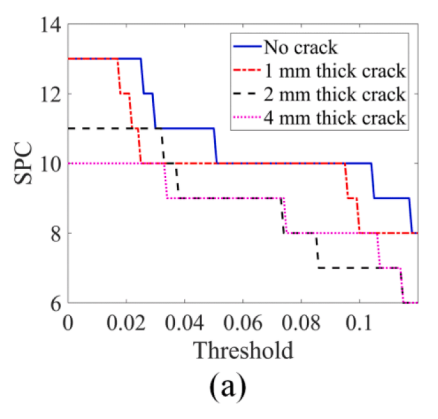


Fig. A1. For the homogeneous steel plate, shown in Fig. 2b, containing two cracks with different thickness values -0 mm (no crack), 1 mm, 2 mm and 4 mm, the SPC plots with threshold varying from 0 to 12 % of the maximum amplitudes of each spectral plot obtained from path No. 4 are shown in (a) and the SPC-I variations for four paths (No. 1, No. 2, No. 3 and No. 4) are shown in (b).



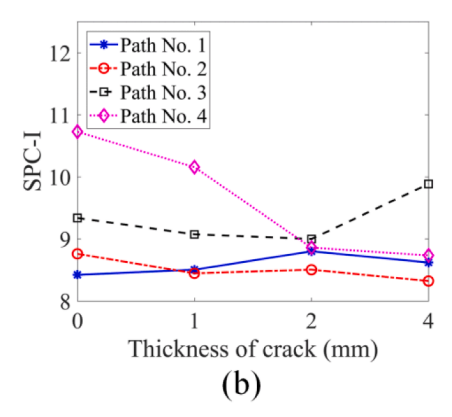
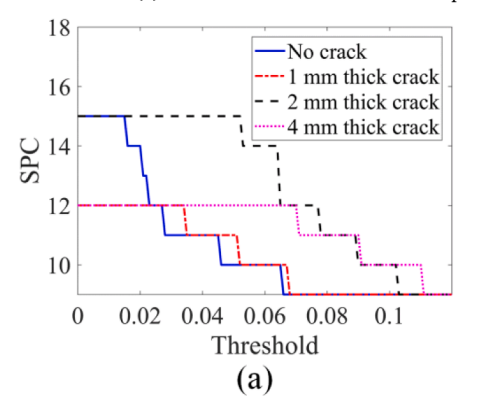


Fig. A2. For the plate containing two cracks of different thicknesses and having "X" topography (vertical aluminum strips in a steel plate as shown in Fig. 4a) the SPC plots for path No. 4 are shown in (a) and the SPC-I variations for four paths are shown in (b).



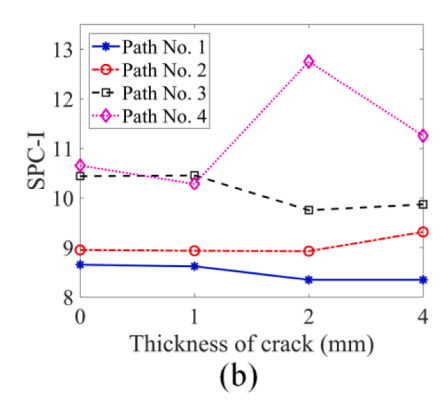
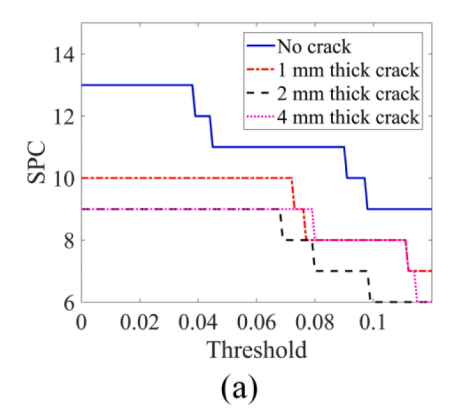


Fig. A3. For the plate containing two cracks of different thicknesses and having "Y" topography (horizontal aluminum strips in a steel plate as shown in Fig. 4b) the SPC plots for path No. 4 are shown in (a) and the SPC-I variations for four paths are shown in (b).



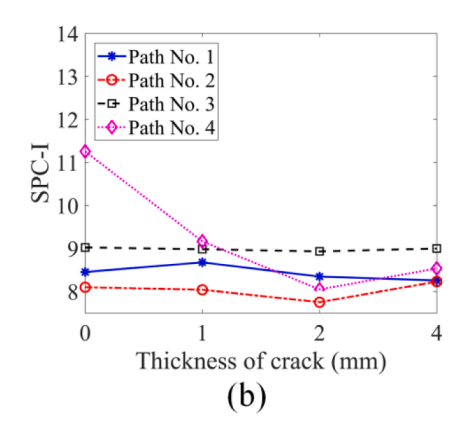


Fig. A4. For the plate containing two cracks of different thicknesses and having "XY" topography (both horizontal and vertical aluminum strips in a steel plate as shown in Fig. 4c) the SPC plots for path No. 4 are shown in (a) and the SPC-I variations for four paths are shown in (b).

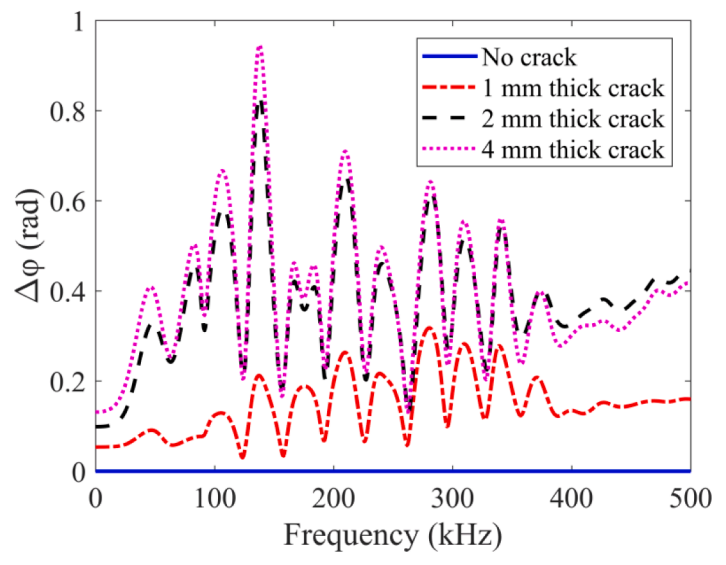


Fig. A5. Geometric phase change as a function of frequency as the crack thickness increases in the homogeneous steel plate.

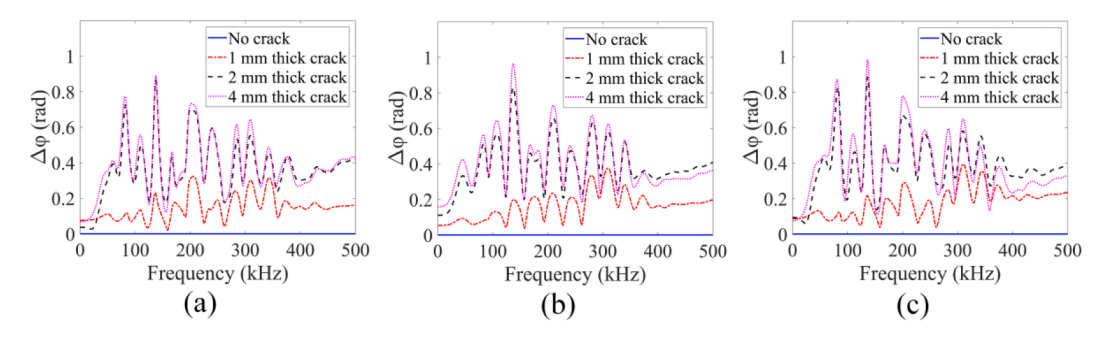
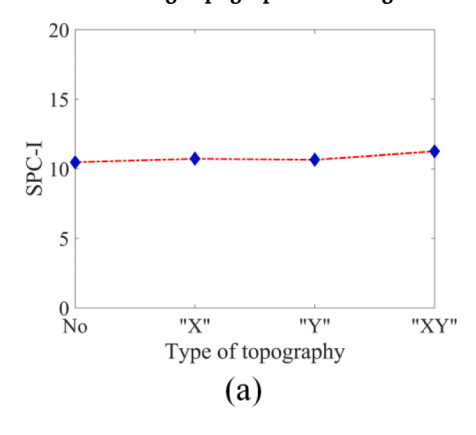


Fig. A6. Geometric phase changes as a function of frequency as the crack thickness increases in plates having (a) "X" topography, (b) "Y" topography and (c) "XY" topography.

Appendix B. Results of sensing topographical changes in steel plates



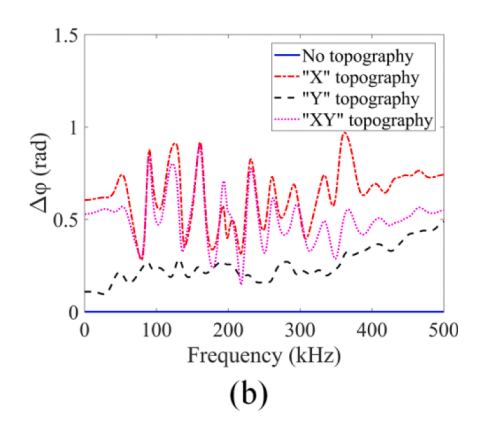


Fig. B1. Sensing results for different topographies in steel plates (a) SPC-I variations and (b) geometric phase changes.

References

- P. Kot, M. Muradov, M. Gkantou, et al., Recent advancements in non-destructive testing techniques for structural health monitoring, Appl. Sci. 11 (6) (2021) 2750.
- [2] F.J. Pallarés, M. Betti, G. Bartoli, et al., Structural health monitoring (SHM) and Nondestructive testing (NDT) of slender masonry structures: A practical review, Constr. Build. Mater. 297 (2021) 123768.
- [3] C. Zhang, W. Li, M. Deng, Investigation of energy trapping effect for nonlinear guided waves in a topographical structure, Appl. Acoust. 214 (2023) 109694.
- [4] X. Yuan, W. Li, M. Deng, Quantitative assessment of corrosion-induced wall thinning in L-shaped bends using ultrasonic feature guided waves, Thin-Walled Struct. (2023) 111493.
- [5] Zhang G, Li X, Li T, et al. Monitoring elastoplastic deformation in ductile metallic materials using sideband peak count-index (SPC-I) technique. Journal of Nondestructive Evaluation, Diagnostics and Prognostics of Engineering Systems, 2023: 1-15.
- [6] H.N. Alnuaimi, S. Sasmal, U. Amjad, et al., Monitoring concrete curing by linear and nonlinear ultrasonic methods, ACI Mater. J. 118 (3) (2021).
- [7] S. Basu, A. Thirumalaiselvi, S. Sasmal, et al., Nonlinear ultrasonics-based technique for monitoring damage progression in reinforced concrete structures, Ultrasonics 115 (2021) 106472.
- [8] T. Arumaikani, S. Sasmal, T. Kundu, Detection of initiation of corrosion induced damage in concrete structures using nonlinear ultrasonic techniques, J. Acoust. Soc. Am. 151 (2) (2022) 1341–1352.
- [9] Castellano A, Fraddosio A, Piccioni M D, et al. Linear and nonlinear ultrasonic techniques for monitoring stress-induced damages in concrete. Journal of Nondestructive Evaluation, Diagnostics and Prognostics of Engineering Systems, 2021, 4(4): 041001.
- [10] H. Alnuaimi, U. Amjad, P. Russo, et al., Monitoring damage in composite plates from crack initiation to macro-crack propagation combining linear and nonlinear ultrasonic techniques, Struct. Health Monit. 20 (1) (2021) 139–150.
- [11] H. Alnuaimi, U. Amjad, S. Park, et al., An improved nonlinear ultrasonic technique for detecting and monitoring impact induced damage in composite plates, Ultrasonics 119 (2022) 106620.
- [12] Alnuaimi H N, Amjad U, Russo P, et al. Advanced non-linear ultrasonic sideband peak count-index technique for efficient detection and monitoring of defects in composite plates. Journal of Vibration and Control, 2023: 10775463231168228.
- [13] P. Liu, H. Sohn, T. Kundu, et al., Noncontact detection of fatigue cracks by laser nonlinear wave modulation spectroscopy (LNWMS), NDT and E Int. 66 (2014) 106–116.
- [14] J.N. Eiras, T. Kundu, M. Bonilla, et al., Nondestructive monitoring of ageing of alkali resistant glass fiber reinforced cement (GRC), J. Nondestr. Eval. 32 (2013) 300–314.
- [15] S. Sasmal, S. Basu, C.V.V. Himakar, et al., Detection of interface flaws in Concrete-FRP composite structures using linear and nonlinear ultrasonics based techniques, Ultrasonics 132 (2023) 107007.
- [16] P. Liu, L. Yang, K. Yi, et al., Application of nonlinear ultrasonic analysis for in situ monitoring of metal additive manufacturing, Struct. Health Monit. 22 (3) (2023) 1760–1775
- [17] Park S H, Alnuaimi H, Hayes A, et al. Nonlinear acoustic technique for monitoring porosity in additively manufactured parts. Journal of Nondestructive Evaluation, Diagnostics and Prognostics of Engineering Systems, 2022, 5(2): 021008.
- [18] Z. Lan, W. Li, M. Deng, et al., Combined harmonic generation of feature guided waves mixing in a welded joint, Wave Motion 117 (2023) 103103.

- [19] Jiang C, Li W, Ng C T, et al. Quasistatic component generation of group velocity mismatched guided waves in tubular structures for microdamage localization. Available at SSRN 4398162.
- [20] S.H. Park, T. Kundu, A modified sideband peak count based nonlinear ultrasonic technique for material characterization, Ultrasonics 128 (2023) 106858.
- [21] G. Zhang, X. Li, T. Kundu, Ordinary state-based peri-ultrasound modeling to study the effects of multiple cracks on the nonlinear response of plate structures, Ultrasonics 133 (2023) 107028.
- [22] S.A. Silling, Reformulation of elasticity theory for discontinuities and long-range forces, J. Mech. Phys. Solids 48 (1) (2000) 175–209.
- [23] S.A. Silling, M. Epton, O. Weckner, et al., Peridynamic states and constitutive modeling, J. Elast. 88 (2007) 151–184.
- [24] Martowicz A, Packo P, Staszewski W J, et al. Modelling of nonlinear Vibro-acoustic wave interaction in cracked aluminum plates using local interaction simulation approach[C]//6th European Congress on Computational Methods in Applied Sciences and Engineering, Vienna, Austria. 2012.
- [25] P.P. Delsanto, M. Scalerandi, A spring model for the simulation of the propagation of ultrasonic pulses through imperfect contact interfaces, J. Acoust. Soc. Am. 104 (5) (1998) 2584–2591.
- [26] Y. Shen, C.E.S. Cesnik, Modeling of nonlinear interactions between guided waves and fatigue cracks using local interaction simulation approach, Ultrasonics 74 (2017) 106–123.
- [27] Y. Shen, C.E.S. Cesnik, Nonlinear scattering and mode conversion of Lamb waves at breathing cracks: An efficient numerical approach, Ultrasonics 94 (2019) 202–217.
- [28] M.H. Hafezi, R. Alebrahim, T. Kundu, Peri-ultrasound for modeling linear and nonlinear ultrasonic response, Ultrasonics 80 (2017) 47–57.
- [29] M.H. Hafezi, T. Kundu, Peri-ultrasound modeling for surface wave propagation, Ultrasonics 84 (2018) 162–171.
- [30] Hadi Hafezi M, Kundu T. Peri-ultrasound modeling of dynamic response of an interface crack showing wave scattering and crack propagation. Journal of Nondestructive Evaluation, Diagnostics and Prognostics of Engineering Systems, 2018, 1(1): 011003-011003-6.
- [31] G. Zhang, X. Li, S. Zhang, et al., Sideband peak count-index technique for monitoring multiple cracks in plate structures using ordinary state-based periultrasound theory, J. Acoust. Soc. Am. 152 (5) (2022) 3035–3048.
- [32] G. Zhang, X. Li, T. Li, et al., Ordinary state-based peri-ultrasound modeling for monitoring crack propagation in plate structures using sideband peak count-index technique, J. Sound Vib. 568 (2024) 117962.
- [33] T.D. Lata, P.A. Deymier, K. Runge, et al., Topological acoustic sensing of spatial patterns of trees in a model forest landscape, Ecol. Model. 419 (2020) 108964.
- [34] T.D. Lata, P.A. Deymier, K. Runge, et al., Topological acoustic sensing of ground stiffness: Presenting a potential means of sensing warming permafrost in a forest, Cold Reg. Sci. Technol. 199 (2022) 103569.
- [35] T.D. Lata, P.A. Deymier, K. Runge, et al., Topological acoustic sensing using nonseparable superpositions of acoustic waves, Vibration 5 (3) (2022) 513–529.
- [36] M.A. Hasan, P.A. Deymier, Modeling and simulations of a nonlinear granular metamaterial: Application to geometric phase-based mass sensing, Model. Simulation Mater. Sci. Eng. 30 (7) (2022) 074002.
- [37] T.D. Lata, P.A. Deymier, K. Runge, et al., Underwater acoustic sensing using the geometric phase, J. Acoust. Soc. Am. 154 (5) (2023) 2869–2877.
- [38] S. Banerjee, Metamaterials in Topological Acoustics, CRC Press, 2023.
- [39] G. Zhang, B. Hu, H. Alnuaimi, et al., Numerical modeling with experimental verification investigating the effect of various nonlinearities on the sideband peak count-index technique, Ultrasonics (2024) 107259.
- [40] Hong M, Su Z, "Chapter 18", Characterizing fatigue cracks using active sensor networks, in: T. Kundu, ed., Springer Nature, Switzerland, 2019, pp. 699–739.